

# Pulse Radiolysis and Laser Flash Photolysis Studies of the Lignin Model $\alpha$ -(*p*-Methoxyphenoxy)-*p*-methoxyacetophenone and Related Compounds

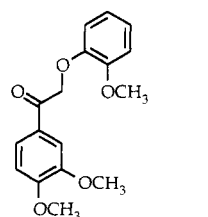
J. C. Scaiano,<sup>\*,†</sup> M. K. Whittlesey,<sup>†</sup> A. B. Berinstain,<sup>†</sup> P. R. L. Malenfant,<sup>†</sup> and R. H. Schuler<sup>†</sup>

Department of Chemistry, University of Ottawa, Ottawa, Canada K1N 6N5, and Radiation Laboratory, University of Notre Dame, Notre Dame, Indiana 46556

Received November 23, 1993. Revised Manuscript Received March 10, 1994\*

The reactivity of reaction intermediates derived from  $\alpha$ -(*p*-anisyl)-*p*-methoxyacetophenone (IIa) and related compounds has been studied in solution and in the solid state, by a combination of laser photolysis techniques, pulse radiolysis, X-ray crystallography, solid-state NMR, emission spectroscopy, molecular modeling, and product studies. In solution the photolysis of IIa proceeds predominantly through the nonfluorescent singlet state that fragments to yield *p*-CH<sub>3</sub>OC<sub>6</sub>H<sub>4</sub>O<sup>•</sup> (VI) and *p*-CH<sub>3</sub>OC<sub>6</sub>H<sub>4</sub>COCH<sub>2</sub><sup>•</sup> (VII) radicals. The latter shows an absorption band at 540 nm. Molecular modeling calculations support the presence of this band and provide a rationalization for this absorption. In the solid state IIa is essentially photostable. The long-lived triplet state decays exclusively by second-order kinetics (triplet-triplet annihilation). In solution the ketyl radical derived from IIa fragments rapidly to yield VI and CH<sub>3</sub>OC<sub>6</sub>H<sub>4</sub>C(OH)=CH<sub>2</sub> with a lifetime of <20 ns. In the context of the lignin photodegradation processes responsible for the yellowing of lignin-rich papers, these results imply that the fragmentation of both the triplet state of IIa and ketyl radicals derived from alcohol groups in lignin will be very difficult to inhibit. Prevention of discoloration is more likely to succeed if the radicals produced from the fragmentations mentioned above are targeted for scavenging before they undergo the oxidative processes that promote yellowing.

During the past few years considerable effort has been devoted to the understanding of the chemistry, particularly the photochemistry, of lignin model compounds.<sup>1</sup> In general, such models aim at reproducing the basic chemical steps that in native lignin lead to its degradation and, in turn, the discoloration of lignin-rich paper and related products. Given the complexity of lignin, a low molecular weight model can reproduce only a few of its key structural features. In our laboratories, research efforts have concentrated on the photochemistry of aromatic carbonyl compounds containing various types of methoxy and phenoxy substitution. A favorite choice of research groups involved in this work has been  $\alpha$ -guaiacoxycetoveratrone, I, a molecule that has been shown to mimic well the light-induced yellowing of lignin.<sup>2-7</sup>



Understanding the photochemistry of these molecules requires knowledge of their excited-state behavior and of the chemical and physical properties of the free radicals derived from these model compounds. Particularly in the case of lignin model compounds, the effect of restricted mobility on these processes is also important. All these aspects have received attention over the last few years and have led to rather variable levels of understanding.<sup>1</sup>

Methoxy substitution of the benzoyl chromophore (as in the case of I) appears to favor singlet-state processes,<sup>5,8,9</sup> in contrast with the usual case of acetophenones and benzophenones in which the photochemistry is dominated by the excited triplet state, which is formed with high or near quantitative quantum yields.<sup>10</sup> A typical reaction in these systems is  $\beta$ -cleavage (reaction 1), which, depending upon the substitution mentioned above, may occur from the singlet or triplet states. In the latter case it has been

<sup>†</sup> University of Ottawa.

<sup>\*</sup> University of Notre Dame.

<sup>†</sup> Abstract published in *Advance ACS Abstracts*, April 15, 1994.

(1) A recent book summarizes the research in the area: *Photochemistry of Lignocellulosic Materials*; Heitner, C., Scaiano, J. C., Eds.; ACS Symposium Series, No. 531; American Chemical Society: Washington, 1993.

(2) Vanucci, C.; Fournier de Violet, P.; Bouas-Laurent, H.; Castellan, A. *J. Photochem. Photobiol. A: Chem.* 1988, 41, 251.

(3) Castellan, A.; Colombo, N.; Vanucci, C.; Fournier de Violet, P.; Bouas-Laurent, H. *J. Photochem. Photobiol. A: Chem.* 1990, 51, 451.

(4) Castellan, A.; Zhu, J. H.; Colombo, N.; Nourmamode, A.; Davidson, R. S.; Dunn, L. *J. Photochem. Photobiol. A: Chem.* 1991, 58, 263.

(5) Schmidt, J. A.; Berinstain, A. B.; de Rege, F.; Heitner, C.; Johnston, L. J.; Scaiano, J. C. *Can. J. Chem.* 1991, 69, 104.

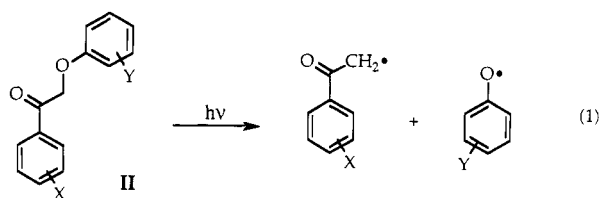
(6) Berinstain, A. B.; Whittlesey, M. K.; Scaiano, J. C. In *Photochemistry of Lignocellulosic Materials*; Heitner, C., Scaiano, J. C., Eds.; American Chemical Society: Washington, 1993; Vol. 531, p 111.

(7) Scaiano, J. C.; Berinstain, A. B.; Whittlesey, M. K.; Malenfant, P. R. L.; Bensimon, C. *Chem. Mater.* 1993, 5, 700.

(8) Palm, W. U.; Dreeskamp, H. *J. Photochem. Photobiol. A: Chem.* 1990, 52, 439.

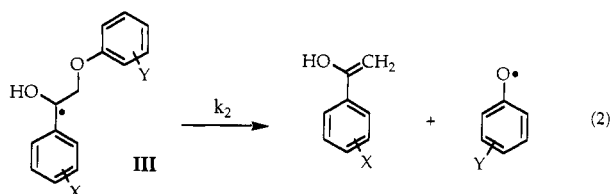
(9) Palm, W. U.; Dreeskamp, H.; Bouas-Laurent, H.; Castellan, A. *Ber. Bunsen-Ges. Phys. Chem.* 1992, 96, 50.

(10) Turro, N. J. *Modern Molecular Photochemistry*; Benjamin/Cummings Publishing Co.: Menlo Park, CA, 1978; p 628.

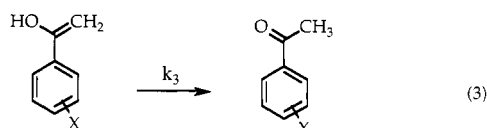


emonstrated that the kinetics of the process are controlled by the stability of the nascent phenoxyl radical.<sup>11</sup>

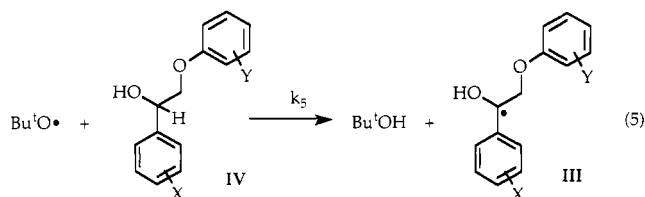
In addition to excited state-cleavage, the ketyl radicals derived from these ketones may undergo their own cleavage reaction, reaction 2.<sup>12</sup> This is then normally followed by



the subsequent reketonization of the enol, i.e.

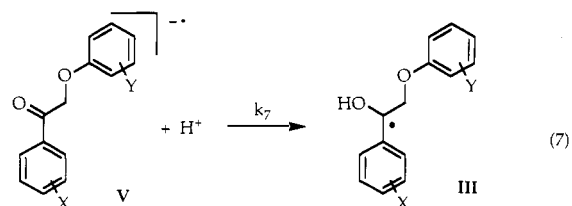
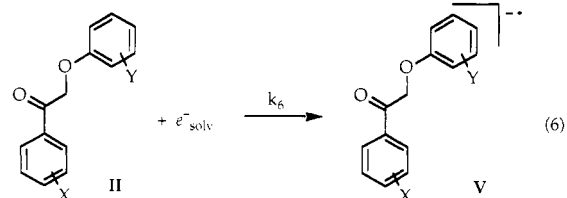


In a recent communication from our laboratory, we have shown that in simple systems (e.g., X = Y = H) reaction 2 occurs with a rate constant  $k_2 > 2 \times 10^6 \text{ s}^{-1}$ .<sup>12</sup> The technique employed involved the generation of the radicals (III) by reaction of photogenerated *tert*-butoxyl radicals with the corresponding alcohol according to reactions 4 and 5.

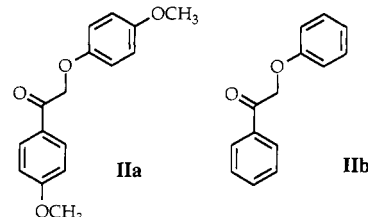


Unfortunately, the time resolution that can be achieved using this approach is limited by the rate of hydrogen abstraction ( $k_5$ ). The rate constant for reaction 5 and the concentration of precursor employed in our earlier work limited the time resolution to approximately 0.5  $\mu\text{s}$ . Further, the process can be complicated in some systems by lack of specificity of the *tert*-butoxyl radicals abstracting hydrogen atoms from other locations in IV.

We reasoned that the time resolution could be significantly improved by finding an alternate source of the ketyl radicals. Electron trapping by the parent ketone followed by radical anion protonation seemed a reasonable alternative to the slower photoinduced routes employed before:<sup>13</sup>



The present study centers on ketone IIa, although some experiments have also been performed with unsubstituted ketone IIb and the widely studied model compound I.



Our report incorporates studies carried out using a variety of spectroscopic techniques including laser flash photolysis, pulse radiolysis, and time-resolved diffuse reflectance measurements. These studies are also complemented by X-ray crystallographic data and solid-state NMR spectra for IIa. The solution photochemistry of I and IIb, as well as the solid-state photolysis of I have been reported previously.<sup>7</sup>

## Results

**Laser Photolysis Studies in Solution.** Pulsed laser excitation (308 nm) of IIa ( $2.3 \times 10^{-4} \text{ M}$ ) in methanol leads to the transient spectra shown in Figure 1. The spectra at different times clearly reveal the presence of at least two species, one absorbing predominantly at 410 nm and the other at  $\sim 540 \text{ nm}$ . The latter disappears more rapidly. Further, it is evident that the 540 nm species must also absorb at wavelengths around 400 nm or shorter; this is indicated by the time-dependent shift to longer wavelengths of the minimum observed between 350 and 400 nm. A similar transient spectrum appears in acetonitrile solution, although the visible band is somewhat blue shifted ( $\lambda_{\text{max}} \sim 500 \text{ nm}$ ). Similar results were obtained upon changing the excitation wavelength from 308 to 337 nm.

The band at 410 nm can be assigned to the phenoxyl radical VI on the basis of experiments where the radical was generated independently by reaction of *tert*-butoxyl radicals (generated by 337 nm photolysis of a 50% solution of *tert*-butyl peroxide in acetonitrile) with *p*-methoxyphenol. An extinction coefficient of  $7030 \text{ M}^{-1} \text{ cm}^{-1}$  at 417 nm has been reported for the radical upon pulse radiolysis of *p*-methoxyphenol in aqueous solution.<sup>14</sup> It is interesting to note that while the guaiacoxyl radical

(11) Netto-Ferreira, J. C.; Avellar, I. G. J.; Scaiano, J. C. *J. Org. Chem.* 1990, 55, 89.

(12) Scaiano, J. C.; Netto-Ferreira, J. C.; Wintgens, V. *J. Photochem. Photobiol. A: Chem.* 1991, 59, 265.

(13) Ross, A. B.; Mallard, W. G.; Helman, W. P.; Bielski, B. H. J.; Buxton, G. V.; Cabelli, D. A.; Greenstock, C. L.; Huie, R. E.; Neta, P. *NRDL/NIST Solution Kinetics Database: Ver. 1; 1.0 ed.*; NIST, U.S. Department of Commerce: Gaithersburg, MD, 1992.

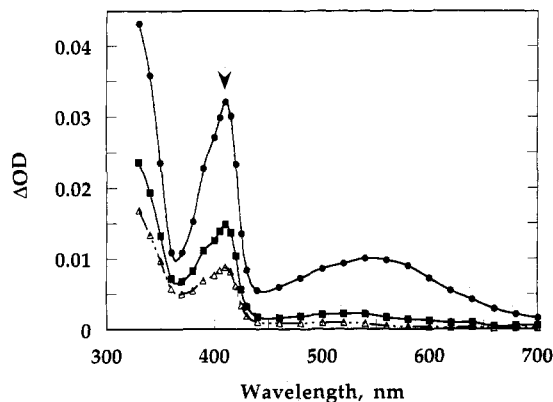
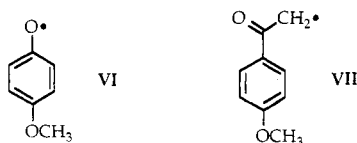


Figure 1. Transient spectra recorded 1.1, 11, and 21  $\mu\text{s}$  following 308-nm laser excitation of **IIa** in methanol.

(the ortho isomer of **VI**) shows a weak but readily detectable band at 660 nm,<sup>6</sup> this band appears to be absent (or to be much weaker) in the case of **VI**.



The complex decay behavior of **VI** appears to approach second-order kinetics; however, concentration studies in which the laser dose was attenuated with neutral density filters suggest a more complex behavior, probably involving reaction with various other radicals present in the system (*vide infra*), as well as some overlap with decay signals associated with the short-wavelength absorptions of the 540-nm transient.

The transient at 540 nm decays with dominant first-order kinetics and a lifetime of  $\sim 7 \mu\text{s}$  in methanol and  $\sim 15 \mu\text{s}$  in acetonitrile. This species is readily scavenged by oxygen, while the band at 410 nm is not affected in the time scale of our experiments. We assign the 540-nm transient to the carbon-centered radical (**VII**) produced simultaneously with **VI** in the  $\beta$ -cleavage of **IIa**.

We found rather surprising that **VII** would show such a long-wavelength absorption; however, the observation is not unprecedented.<sup>15</sup> We will show later that not only is this assignment fully consistent with our results, but in addition it is in accord with the spectra predicted by molecular modeling calculations (*vide infra*).

It should be noted that the 410-nm band of Figure 1 is not unlike typical triplet-triplet absorptions from *p*-methoxybenzoyl chromophores.<sup>16,17</sup> However, we feel confident that the transient derived from **IIa** is not due to the triplet and the assignment of this band to **VI** is correct. Note, for example, that the band persists in the presence of oxygen, contrary to what one would expect for a triplet state. Similarly, experiments with 2,5-dimethyl-2,4-hexadiene showed that this typical triplet quencher had no effect on the transient lifetime at 410 nm, and any changes in signal intensity were well below 10% for diene concentrations up to 1.12 M (in acetonitrile). This suggests that if the precursor of **VI** is the triplet state, its lifetime

should be  $\leq 1$  ns. More likely (*vide infra*), a short triplet lifetime and contributions from singlet-state  $\beta$ -cleavage are responsible for the failure of diene quenching experiments. The 540-nm absorption was quenched by diene with a rate constant of  $1.8 \times 10^5 \text{ M}^{-1} \text{ s}^{-1}$ , a value that is in line with radical addition rate constants to conjugated systems.<sup>18</sup> **VII** is also believed to abstract hydrogen from 2-propanol.<sup>19</sup>

To obtain an estimate for the triplet lifetime, we have employed a Stern-Volmer type of approach using 1-methylnaphthalene as a triplet quencher. This technique, which has been previously used in our laboratory in the study of short-lived triplet states,<sup>20</sup> makes use of eq 8, where

$$A_{420} = \alpha + \frac{\alpha}{k_q \tau_T [\text{MN}]} \quad (8)$$

$A_{420}$  is the transient absorption at 420 nm,  $\tau_T$  is the triplet lifetime,  $k_q$  is the quenching rate constant, and  $\alpha$  is an experimental constant. In this case, complications arise due to the absorption at 420 nm of the *p*-methoxyphenoxyl radical itself formed upon direct excitation of ketone **IIa**. The absorption due to the triplet state of 1-methylnaphthalene was therefore corrected by subtracting the contribution due to the singlet-derived radical. The experiment yields a value for  $k_q \tau_T$  of  $2.4 \text{ M}^{-1}$ , indicating a triplet lifetime of  $\sim 500$  ps.<sup>21</sup> We note that lifetimes of this magnitude determined in quenching studies may be the subject of some error resulting from transient quenching effects.<sup>22</sup>

Experiments with **IIa** in sodium dodecyl sulfate (SDS) micelles [**IIa** =  $2 \times 10^{-4} \text{ M}$ , SDS = 0.1 M] yield a transient spectrum with a strong absorption at  $\sim 700$  nm and a band at  $\sim 410$  nm. The long-wavelength band, which is fully quenched with nitrous oxide,<sup>23</sup> is assigned to the solvated electron;<sup>13</sup> further details of this chemistry will be reported elsewhere.<sup>24</sup> Nitrous oxide has no effect on the band at 410 nm, although the quenching of the absorption at 700 nm indicates that there is no significant band present in the 550-nm region. Application of moderate magnetic fields ( $\leq 1200$  G) had no effect on the decay kinetics at 410 nm on short time scales ( $\leq 2 \mu\text{s}$ ). Significant effects could be anticipated if the cleavage generated a triplet radical pair.<sup>25-28</sup> The absence of magnetic field effects on this time scale is consistent with the dominance of singlet cleavage pathways.

**Pulse Radiolysis Studies.** The reactions of solvated electrons with **IIa** and **IIb** were examined using pulse radiolysis techniques employing the facility at the Notre

(18) Korus, R.; O'Driscoll, K. F. In *Polymer Handbook*, 2nd ed.; Brandrup, J., Immergut, E. H., McDowell, W., Eds.; Wiley-Interscience: New York, 1975; pp II-45.

(19) Tsunooka, M.; Tanaka, S.; Tanaka, M. *Makromol. Chem., Rapid Commun.* 1983, 4, 539.

(20) Netto-Ferreira, J. C.; Leigh, W. J.; Scaiano, J. C. *J. Am. Chem. Soc.* 1985, 107, 2617.

(21) Lissi, E. A.; Encinas, M. V. In *Handbook of Organic Photochemistry*; Scaiano, J. C., Ed.; CRC Press: Boca Raton, FL, 1989; Vol. II, p 111.

(22) Noyes, R. M. *Prog. React. Kinet.* 1961, 1, 131.

(23) Bensasson, R. V.; Land, E. J.; Truscott, T. G. *Flash Photolysis and Pulse Radiolysis*; Pergamon Press: New York, 1983.

(24) Boch, R.; Whittlesey, M. K.; Scaiano, J. C., submitted.

(25) Scaiano, J. C.; Abuin, E. B.; Stewart, L. C. *J. Am. Chem. Soc.* 1982, 104, 5673.

(26) Evans, C.; Ingold, K. U.; Scaiano, J. C. *J. Phys. Chem.* 1988, 92, 1257.

(27) Gould, I. R.; Zimmt, M. B.; Turro, N. J.; Baretz, B. H.; Lehr, G. *J. Am. Chem. Soc.* 1985, 107, 4607.

(28) Cozens, F. L.; Scaiano, J. C. *J. Am. Chem. Soc.* 1993, 115, 5204.

(14) Alfassi, Z. B.; Schuler, R. H. *J. Phys. Chem.* 1985, 89, 3359.

(15) Fouassier, J. P.; Burr, D. *Macromolecules* 1990, 23, 3615.

(16) Carmichael, I.; Hug, G. L. *J. Phys. Chem. Ref. Data* 1986, 15, 1.

(17) Carmichael, I.; Hug, G. L. In *Handbook of Organic Photochemistry*; Scaiano, J. C., Ed.; CRC Press: Boca Raton, FL, 1989; Vol. I, p 369.

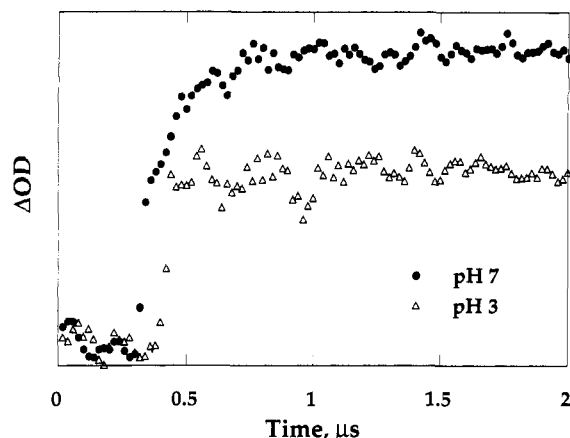


**Figure 2.** Pulse radiolysis traces showing the formation of VI from IIa at pH 7 and 3. Monitored at 415 nm.

Dame Radiation Laboratory. Experiments were performed in water-alcohol mixtures (70:30 v/v) which offer suitable properties in terms of ketone solubility and allow the pH of the solution to be adjusted.

Under pulse radiolysis conditions in methanol/water mixtures, the ketone can be reduced to the radical anion by reaction with solvated electrons (see reaction 6). The anion can in turn be protonated by the solvent to form the ketyl radical according to reaction 7.

In experiments of this type the solvated electron can be readily monitored since it has a strong absorption in the red region ( $>600$  nm). In our case it was possible to determine a rate constant for reaction of  $e^-_{\text{solv}}$  with IIa by monitoring the electron decay at 550 nm using 1 mM ketone. These experiments led to  $k_7 = 1.9 \times 10^{10} \text{ M}^{-1} \text{ s}^{-1}$ , a value that is in line with reported rate constants for electron scavenging by ketones.<sup>13</sup> For example, acetophenone scavenges hydrated electrons with a rate constant of  $2.8 \times 10^{10} \text{ M}^{-1} \text{ s}^{-1}$ .<sup>13</sup>

In the experiments described below the concentration of IIa was fixed at 10 mM, which ensures the prompt formation of the anion, which under these conditions should occur with a lifetime  $\leq 6$  ns.

The protonation of the anion can be the rate-determining step for the formation of the phenoxyl radical. This is illustrated in Figure 2 which shows traces at 415 nm following pulse radiolysis of IIa in alcohol-water at pH 7 and 3. The trace at pH 7 shows an initial jump due to the absorption of the anion (Va), followed by a growth with a lifetime of  $\sim 100$  ns. We had hoped that as the pH was lowered and the protonation became formally "instantaneous", we would be able to monitor the lifetime of the ketyl radical (IIIa) either through its direct detection, or by studying the growth kinetics for the *p*-methoxyphenoxyl radical (VI). While the phenoxyl radical was indeed readily detectable (see Figure 3), we were unable to study the time dependence of reaction 7, which under our experimental conditions must occur with  $k_7 > 5 \times 10^7 \text{ s}^{-1}$ . Note for example that the trace at pH 3 in Figure 2 represents an instantaneous growth in the time scale of the experiments.

Experiments with IIb yielded less definitive results. Irradiation of IIb in 70:30 methanol:water v/v ([IIb] = 10 mM) produced a transient spectrum with  $\lambda_{\text{max}}$  at ca. 440 nm. The growth of this species appeared to be instantaneous and it decayed with pseudo-first-order kinetics ( $k_{\text{obs}} = 1.15 \times 10^6 \text{ s}^{-1}$ ) to leave a residual absorption which

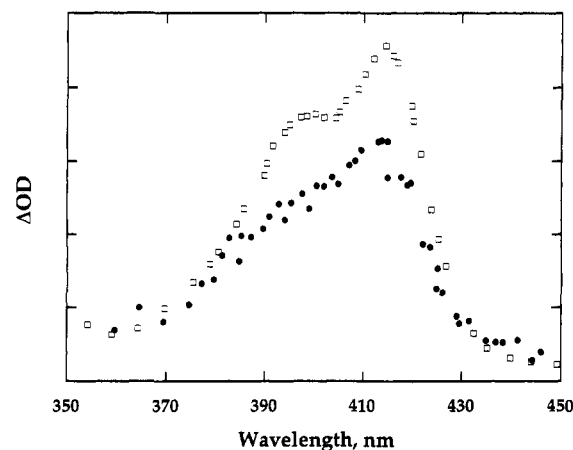


**Figure 3.** Transient spectra for VI generated by ( $\square$ ) pulse radiolysis of IIa and ( $\bullet$ ) control experiment where VI was generated independently from the reaction corresponding of *tert*-butoxy radicals with the phenol.

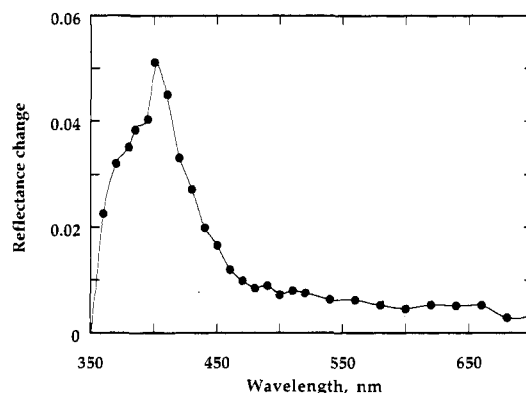


**Figure 4.** Solid-state transient spectra from crystalline IIa, obtained by 308-nm laser excitation and using time-resolved diffuse reflectance to monitor the signals. Spectrum recorded 0.5  $\mu\text{s}$  after the laser pulse.

has no clear maximum in this region of the spectrum. Monitoring the decay of the electron at 550 nm with a 1 mM solution of IIb yielded a similar scavenging rate constant as for IIa ( $k_2 = 1.3 \times 10^{10} \text{ M}^{-1} \text{ s}^{-1}$ ). Lowering the pH to 3.3 resulted in the disappearance of the decay at 440 nm and the instant formation of the residual.

**Laser and Lamp Excitation of IIa in the Solid State.** Lamp irradiation of a sample of IIa (0.2 g) with 9 RPR-300 lamps for 7 days under nitrogen followed by dissolution in methanol and chromatographic analysis did not lead to any significant yields of new products, although the sample was significantly yellow after the photolysis. Thus, under these irradiation conditions IIa is essentially photostable, just as I has been demonstrated to be in earlier work.<sup>7</sup>

In contrast with the negative results of product studies, 308-nm laser excitation of crystals of IIa gives a transient spectrum (monitored using diffuse reflectance detection) with  $\lambda_{\text{max}}$  390 nm (Figure 4). At this wavelength, the transient decays with perfect second-order kinetics, as illustrated in Figure 5, which shows both the second-order fit and (inset) a representative decay trace. As is frequently the case with diffuse reflectance studies, the signal intensity did not increase linearly with laser power, although the decay of the transient followed clean second-order kinetics at all powers.

The transient of Figures 4 and 5 is assigned to the triplet state of IIa. The reasons which support this assignment

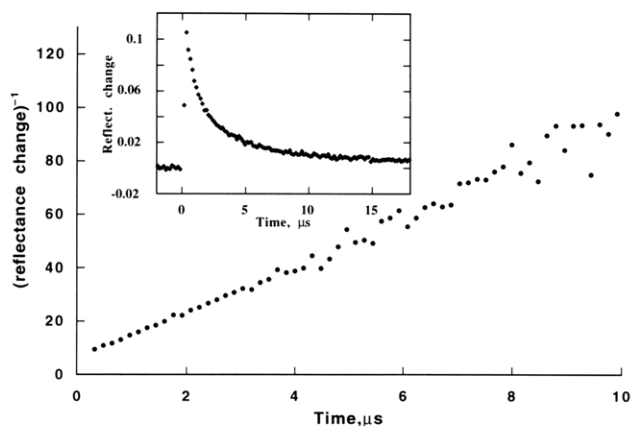


**Figure 5.** Inset: a diffuse reflectance decay trace recorded at 400 nm following 308-nm excitation of crystalline **IIa**. The main plot shows a second-order kinetic fit of the data.

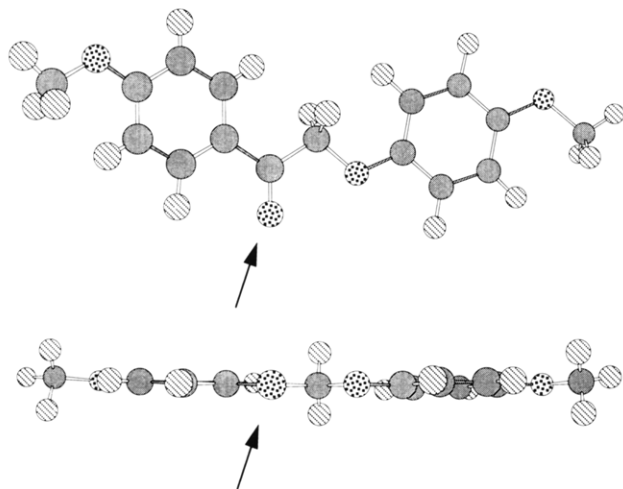


**Figure 6.** Two views of the structure of **IIa** as determined by X-ray crystallography. In the top view the carbonyl group (note arrow) has been aligned with the Z axis, and in the bottom view with the Y axis. Note that **IIa** is essentially planar.

(as opposed to free radicals) will be reviewed in detail in the Discussion. No difference in the signals (spectrum or kinetics) was detected regardless of whether the crystals were irradiated under oxygen or under nitrogen.

**NMR and X-ray Crystallographic Studies of IIa.** The  $^{13}\text{C}$  NMR spectrum of **IIa** in  $\text{CDCl}_3$  solution showed a single carbonyl resonance at  $\delta$  193.3 ppm. Solid-state  $^{13}\text{C}$  CP-MAS NMR revealed a single carbonyl signal at  $\delta$  188.9 ppm. We have previously reported solid-state studies on **I** in which the  $^{13}\text{C}$  CP-MAS NMR spectrum showed three carbonyl resonances.<sup>7</sup> In conjunction with this, X-ray crystallographic data showed the presence of four distinct molecules of **I** in the unit cell although two of these are sufficiently similar that they are not differentiated in the CP-MAS NMR spectrum. Further details on the NMR data are provided in the Experimental Section.

The crystallographic studies on **IIa** indicate monoclinic crystals with a unit cell ( $10.68 \text{ \AA} \times 9.27 \text{ \AA} \times 13.53 \text{ \AA}$ ) containing four molecules of **IIa**, but all in identical conformations, as illustrated in Figure 6. This stretching conformation is totally unsuitable for  $\beta$ -phenyl quenching, a common form of decay for ketones of this type.<sup>11,20,29</sup> Figure 7 shows a stereodiagram of the unit cell illustrating

the relative positioning of molecules of **IIa** in the crystal. The planes of the aromatic rings in the crystal are located at distances ranging from 3.4 to 3.6  $\text{\AA}$ , but the *p*-methoxybenzyl rings are somewhat shifted relative to each other. While in the case of **I** we found that intermolecular interactions led to efficient singlet interaction and deactivation, this seems not to be the case for **IIa** which succeeds in populating the triplet manifold.

**Molecular Modeling Calculations on Radicals Resulting from  $\beta$ -Cleavage.** We were concerned and surprised at the long-wavelength absorption of **VII**. This led us to carry out calculations on **VII** and related radicals. These systematically indicate the presence of a band in the 500-nm region and suggest considerable delocalization in the radical.

Minimized structures for the benzoylmethyl radicals from **IIa**, **IIb**, and **I** were calculated using the PM3 semiempirical SCF-MO method as implemented in a version of the MOPAC program.<sup>30,31</sup> The calculated C=O bond order in the *p*-methoxybenzoylmethyl radical is 1.66, suggesting a significant contribution from the canonical form of the radical in which the unpaired electron is centered on the oxygen atom.

The corresponding electronic absorption spectra were determined by the CI/ZINDO method. The predicted spectra each showed a weak feature at  $\sim 520 \text{ nm}$  along with a stronger band at  $\sim 400 \text{ nm}$  (Figure 8). The transition largely responsible for the 520 nm band in the *p*-methoxybenzoylmethyl radical is from (HOMO-1) to LUMO, involving delocalization of electron density out over the carbonyl moiety. The orbitals are shown in Figure 8.

## Discussion

While this contribution covers many aspects of the structure, photochemistry and behavior of derived radicals from **IIa** and related substrates, perhaps the most important observation in relation to lignin processes is that ketyl radicals, such as **III**, undergo the fragmentation reaction very rapidly; in fact reaction 3 is even faster than suggested by previous work, with a rate constant in excess of  $5 \times 10^7 \text{ M}^{-1} \text{ s}^{-1}$  in the case of **IIa** ( $X = Y = p\text{-CH}_3\text{O}$ ). The implication for lignin photochemistry is that ketyl radicals of this type, if formed, will cleave to produce phenoxyl radicals fast, efficiently, and with little probability of scavenging them before cleavage. Thus, if radicals are to be intercepted as a way of preventing yellowing of lignin-rich products, the ketyl radicals should not be the preferred targets for such scavenging.

Our studies also confirm that at least in the case of methoxy substituted systems, such as **IIa**, excited state fragmentation (reaction 1) occurs extensively from the singlet state. The same conclusion was recently reported by Palm et al. for a series of phenoxyacetophenones (including **I**, **IIa**, and **IIb**) employing CIDNP techniques.<sup>8,9</sup> In the case of **IIa** this process is probably assisted by the gain in stability of the *p*-methoxy-substituted phenoxyl radical, in addition to the effect of methoxy substitution on the benzoyl chromophore. Similar arguments apply to **I** which fragments from both singlet and triplet states.<sup>5,32</sup> In the case of **IIa**, quantitative identification of the triplet component is difficult because the short triplet lifetime

(29) Scaiano, J. C.; Casal, H. L.; Netto-Ferreira, J. C. *ACS Symp. Ser.* 1985, 278, 211.

(30) Stewart, J. J. P. *J. Comput. Chem.* 1989, 10, 209.

(31) Stewart, J. J. P. *J. Comput. Chem.* 1989, 10, 221.

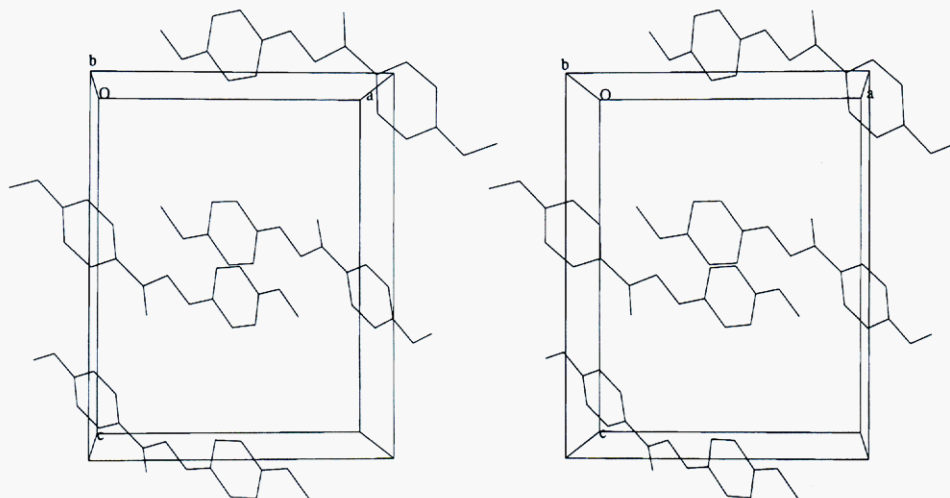


Figure 7. Stereodiagram of the unit cell for **IIa** based on the X-ray crystallographic studies.

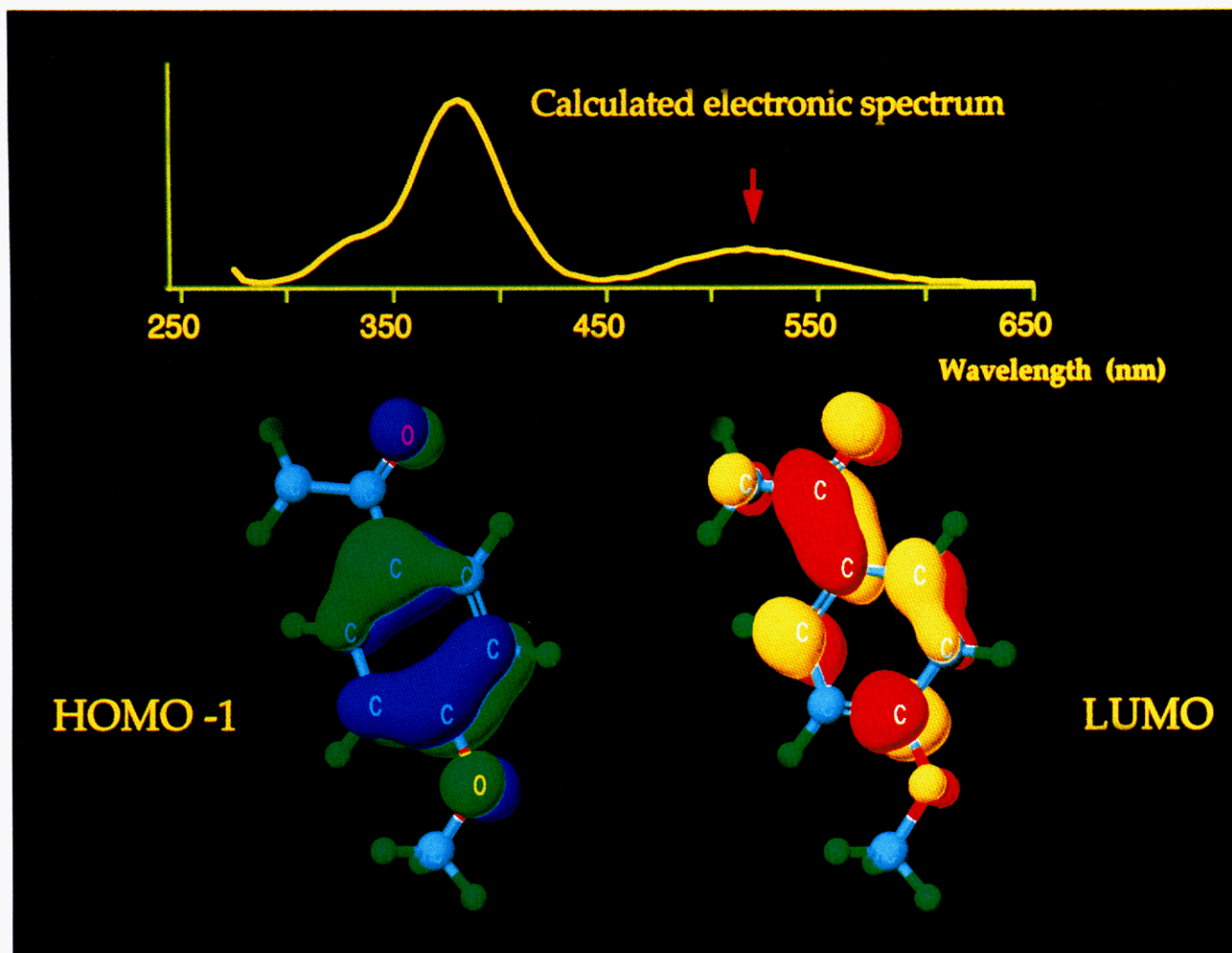


Figure 8. Calculated spectra (CI/ZINDO, see text) for radical **VII**, and (HOMO-1) (left) and LUMO involved in the visible absorption band.

makes distinction between singlet and triplet processes hard to achieve. However, magnetic field studies in SDS micelles appear to confirm the predominance of singlet processes. Again, in the context of lignin degradation in

lignin-rich products, it is hard to see that singlet precursors will be quenched by additives before fragmentation occurs. The radical products from reaction 1 should however be susceptible to trapping.

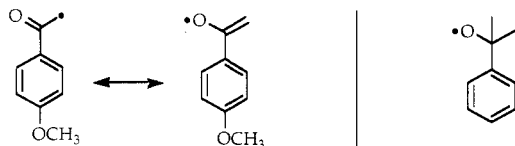
Solution studies on **IIa** suggest relatively clean transient phenomena, with only two transients formed. Given the short lifetimes of the excited states of **IIa**, it seems reasonable to assume that the signals are due to free radical

(32) Schmidt, J. A.; Goldsmidt, E.; Heitner, C.; Scaiano, J. C.; Berinstain, A. B.; Johnston, L. J. In *Photochemistry of Lignocellulosic Materials*; Heitner, C., Scaiano, J. C., Ed.; American Chemical Society: Washington, 1993; Vol. 531, p 122.



products. The *p*-methoxyphenoxy radical can be readily characterized. Firstly, an absorption maximum has been reported in the literature<sup>14</sup> and we have recorded the spectrum in our own pulse radiolysis experiments. Further, we generated it under our laser photolysis conditions by reaction of photogenerated *tert*-butoxyl radicals with the corresponding phenol. This led to  $\lambda_{\text{max}}$  at 405 nm in acetonitrile. We were particularly interested in establishing if this radical had a long-wavelength band, since these are present in some substituted phenoxy radicals but seldom reported. In the case of VI we did not observe any long-wavelength (>450 nm) band, suggesting that such a band, if present must be very weak. This means naturally that the 540 nm absorption must be attributed to another species. This is consistent with the different decay kinetics observed at 410 and 540 nm. We attribute the latter to VII, along with shorter wavelength absorptions that overlap the phenoxy band (*vide infra*). Interestingly, several radicals of the same family are predicted by the CI/ZINDO calculations to have absorption in that region. A visible absorption band for the benzoylmethyl radical was first reported by Shida and co-workers in a low-temperature glass.<sup>33</sup>

A comparison here can also be drawn to the recent results of Ingold and co-workers who have reported bands in the visible region for the cumyloxyl radical (485 nm) and *p*-methoxycumyloxyl radical (590 nm) in acetonitrile solution.<sup>34</sup> One canonical form of the benzoylmethyl radical involves an oxygen centered radical, not too dissimilar to the radicals reported by Ingold:



ESR studies have confirmed the partial C=C double-bond character in both the benzoylmethyl radical<sup>35</sup> and related 2-alkanoxy radicals.<sup>36</sup>

As indicated above, we assign the signals observed in the photolysis of crystalline IIa to its triplet state. We interpret the second-order decay of these signals as resulting from triplet-triplet annihilation following triplet energy migration through the crystal lattice. Further, the spectrum recorded in the crystals is virtually identical to that from triplet *p*-methoxyacetophenone but significantly different (shifted) from that for radical VI. The alternative interpretation that the signals are due to VI is also inconsistent with several experimental facts: (a) If VI was to decay by recombination with VII in a geminate fashion, their decay should follow first-order kinetics. (b) If for any reasons the radical centers migrate, it is hard to imagine how they could fail to yield any new products. (c) If VII was formed, the absence of the 540-nm band would be surprising. The simplest explanation is that intersystem crossing into the triplet manifold is enhanced in crystalline media and that the triplet, being in a

conformation inadequate for  $\beta$ -aryl quenching lives long enough to be readily detectable.

Palm et al.<sup>9</sup> report that IIa does not fluoresce in solution. In the solid state the interplane distance between molecules of IIa is around  $\sim 3.5$  Å. In the solid state the fluorescence maximum is at about 420 nm. Since fluorescence is present in the solid, this points to the fact that the singlet state is sufficiently long lived to allow intersystem crossing to take place.

## Conclusion

Photolysis of IIa in solution leads to its fragmentation into *p*-CH<sub>3</sub>OC<sub>6</sub>H<sub>4</sub>O<sup>•</sup> and *p*-CH<sub>3</sub>OC<sub>6</sub>H<sub>4</sub>COCH<sub>2</sub><sup>•</sup>, in a process that occurs either from the singlet state or from an extremely short lived triplet state; our results favor a singlet mechanism. In contrast with the solution behavior, IIa is photostable in the solid state, where its triplet state can be readily detected.

The ketyl radical (IIIa) fragments to yield *p*-CH<sub>3</sub>-OC<sub>6</sub>H<sub>4</sub>O<sup>•</sup> (VI) and the enol *p*-CH<sub>3</sub>O-C<sub>6</sub>H<sub>4</sub>C(OH)=CH<sub>2</sub> with a rate constant in excess of  $5 \times 10^7$  s<sup>-1</sup>. This appears to be a rather general process in ketyl radicals with lignin-related structures. In pulse radiolysis experiments the formation of VI is limited by the rate of protonation of the keto anion produced by electron capture by the ketone.

In the context of lignin photodegradation two of the processes studied here are too fast for the species involved to be susceptible for scavenging. Specifically, the photofragmentation of IIa and the cleavage of ketyl radicals (reaction 2) are too fast to leave much room for effective trapping. Clearly if the discoloration of lignin rich products can be prevented by scavenging reaction intermediates, other long-lived species (such as VI and VII) will have to be targeted for scavenging.

Molecular modeling calculations and its reactivity, both suggest that the radical produced by cleavage of IIa, *p*-CH<sub>3</sub>-OC<sub>6</sub>H<sub>4</sub>COCH<sub>2</sub><sup>•</sup> has considerable spin density on the carbonyl oxygen, which is also involved in the visible absorption band. These results suggest that VII may behave either as a carbon or an oxygen center radical. These processes are currently being examined in some detail.

## Experimental Section

**Materials.** The solvents methanol (BDH) and acetonitrile (BDH) were Omnisolv grade and used as received. SDS (BDH) was "specially pure" grade and used as received. The quenching 1-methylnaphthalene (Aldrich, 98%) and 2,5-dimethyl-2,4-hexadiene (Aldrich, 99%) were used as received. Di-*tert*-butyl peroxide (Aldrich) was passed through an alumina column immediately before use to eliminate traces of hydroperoxide. *p*-Methoxyphenol (Aldrich, 99%) was recrystallized before use.

The ketone IIa was prepared by reaction of  $\alpha$ -bromo-*p*-methoxyacetophenone with *p*-methoxyphenol using dry acetone as solvent in alkaline media. The most favorable method of preparation involved stirring the phenol in the basic solution for 2 h, followed by dropwise addition of an acetone solution of the ketone. The mixture was then refluxed until a GC trace showed >95% conversion to the required product. Workup involved removal of any excess phenol followed by purification of the ketone by recrystallization from methanol.

IIb was prepared as for IIa using  $\alpha$ -bromoacetophenone and phenol. I was prepared as previously described by Adler et al.<sup>37</sup> Ketones VIII and IX (Aldrich) were recrystallized from methanol before use.

(33) Shida, T.; Iwata, S.; Imamura, M. *J. Phys. Chem.* 1974, 78, 741.

(34) Avila, D. V.; Lusazyk, J.; Ingold, U. *J. Am. Chem. Soc.* 1992, 114, 6576.

(35) Bargon, J.; Graf, F.; Lau, W.; Ling, A. C. *J. Phys. Chem.* 1979, 83, 269.

(36) Camaioni, D. M.; Walter, H. F.; Jordan, J. E.; Pratt, D. W. *J. Am. Chem. Soc.* 1973, 95, 7978.

(37) Adler, E.; Lindgren, B. O.; Saedén, U. *Sven. Papperstidn.* 1952, 55, 245.

Physical and spectroscopic data for **IIa** are reported below. The melting point and  $^1\text{H}$  NMR data recorded was in agreement with data in the literature.<sup>9</sup> **IIa**:  $^{13}\text{C}$  NMR ( $\text{CDCl}_3$ )  $\delta$  193.3 ( $\text{C}=\text{O}$ ), 164.0 ( $-\text{CH}_2\text{OC}-$ ), 154.3 ( $-\text{COCH}_3$ ), 152.3 ( $-\text{COCH}_3$ ), 130.4, 127.6, 115.9, 114.6, 113.9 (aromatic), 71.5 ( $-\text{CH}_2-$ ), 55.6 ( $-\text{OCH}_3$ ), 55.5 ( $-\text{OCH}_3$ ); MS  $m/z$  (%) 272 (54.7), 136 (28.5), 135 (100), 121 (21.8), 107 (21.8), 92 (27), 77 (44.7), 28 (21); IR ( $\text{CH}_2\text{-Cl}_2$ )  $1695\text{ cm}^{-1}$  ( $\nu_{\text{CO}}$ ); UV-vis (MeOH,  $\lambda_{\text{max}}$  (nm),  $\epsilon$  ( $\text{M}^{-1}\text{ cm}^{-1}$ )) 204 (19 800), 224 (17 100), 282 (17 700).

**General Techniques.**  $^{13}\text{C}$  CP-MAS NMR spectra were recorded as previously described.<sup>7</sup>  $^1\text{H}$  and  $^{13}\text{C}$  NMR spectra in solution were recorded using a Varian Gemini 200-MHz spectrometer. GC analysis was carried out on a PE Model 8320 capillary column chromatograph. IR spectra were recorded on a Bomem MB-100 FTIR and UV-vis spectra with a HP-8451A diode array spectrometer. Melting points were determined in a Mel-Temp apparatus and were not corrected.

**Laser Flash Photolysis.** The laser flash photolysis experiments employed either a Lumonics EX-510 excimer laser (308 nm, 30 mJ/pulse, 6-ns pulse width) or a Molelectron UV-24 nitrogen laser (337.1 nm, 5 mJ/pulse, 8-ns pulse width) for excitation. Data were captured by a Tektronix 2440 digital oscilloscope interfaced to a Macintosh IIfx computer operated with LabVIEW 2.2 software. A program written in LabVIEW was responsible for all data acquisition and instrument control. Experiments involving 308 nm irradiation were carried out in  $7 \times 7\text{ mm}^2$  Suprasil quartz cell with  $90^\circ$  excitation. In the case of experiments with the nitrogen laser,  $3 \times 7\text{ mm}^2$  cells were used with front face irradiation. All experiments were carried out under flow conditions and under a nitrogen atmosphere unless otherwise stated.

**Time-Resolved Diffuse Reflectance.** The diffuse reflectance laser flash photolysis system is similar to those described elsewhere.<sup>38</sup> A Lumonics EX-510 excimer laser (XeCl, 308 nm, 30 mJ/pulse, 6-ns pulse width) was used for excitation. The data collection and processing was carried out as above.

**Pulse Radiolysis.** Pulse radiolysis experiments were carried out at the Notre Dame Radiation Laboratory. The solutions were irradiated with 5-ns pulses from an ARCO LP-7 linear accelerator. Computer control of the equipment has been described previously.<sup>14</sup> Digitization of the transient signals was usually with a Biomation 8100. A Biomation 6500 was used for experiments below  $1\text{-}\mu\text{s}$  full scale. Dosimetry experiments were carried out as previously reported.<sup>39</sup>

Solutions of ketones **IIa**, **IIb**, and **I** in 70:30 methanol:water (containing 5–10 mM phosphate buffer) were flowed through the 10-mm path-length irradiation cell under nitrogen. Solutions were prepared with water from a Millipore Milli-Q system and pH adjusted with reagent grade  $\text{HClO}_4$ . The spectrum of the *p*-methoxyphenoxyl radical was recorded upon oxidation of *p*-methoxyphenoxide in basic aqueous solution by  $\text{N}_3$  radicals.

**X-ray Crystallography.** *Data collection:* A crystal of  $\text{O}_4\text{C}_{16}\text{H}_{16}$  having approximate dimensions of  $0.2 \times 0.08 \times 0.25\text{ mm}$  was mounted on a glass capillary. All the measurements were made on a Rigaku diffractometer with  $\text{Mo K}\alpha$  radiation. Crystal data are given in Table 1. Detailed information is available as supplementary material (see paragraph at end of paper).

Cell constants and an orientation matrix for data collection were obtained from least-squares refinement using the setting angles of 25 reflections in the range  $40^\circ < 2\theta < 45^\circ$ ; these corresponded to a monoclinic cell with dimensions  $a = 10.683(2)$ ,  $b = 9.268(3)$ ,  $c = 13.534(3)\text{ \AA}$ ,  $\beta = 90.277(17)^\circ$ . For  $z = 4$  and  $\text{FW} = 272.20$ , the calculated density is  $1.350\text{ g/cm}^3$ . On the basis of the systematic absences, the space group was determined to be  $P2_1/c$ . The data were collected at  $-110^\circ\text{C}$  using the  $\omega$ - $2\theta$  scan technique to a maximum  $2\theta$  value of  $46.9$ .

*Data reduction:* A total of 2093 reflections were collected. The unique set contains only 1974 reflections. The standards were measured after every 150 reflections. No crystal decay was noticed. The data were corrected for Lorentz and polarization effects.<sup>40</sup> No absorption correction was made.

Table 1. Crystal Data on **IIa**

empirical formula	$\text{O}_4\text{C}_{16}\text{H}_{16}$
formula weight	272.20
crystal shape	needle
crystal dimensions (mm)	0.2, 0.08, 0.25
crystal system	monoclinic
no. of refls used for unit cell dimension ( $2\theta$ range)	25
lattice parameters	$a = 10.683(2)$ $b = 9.268(3)$ $c = 13.534(3)$ $\beta = 90.277(17)$
space group	$P2_1/c$
Z value	4
$D_{\text{calc}}$ ( $\text{g}\cdot\text{cm}^{-3}$ )	1.350
$F(000)$	576.26
$\mu$ ( $\text{mm}^{-1}$ )	0.09
no. of refls measured	2093
no. of refls unique	1974
no. of refls observed	1469
no. of atoms	36
no. of variables	246
$R_f$ (sign refl)	0.053
$R_w$ (sign refl)	0.033
$R_f$ (all refl)	0.079
$R_w$ (all refl)	0.034
goodness of fit	4.70
last difference Fourier map	
max peak	0.220
min peak	-0.230

**Solution and refinement:** The structure was solved by direct methods. All the atoms were refined anisotropically except the hydrogen. The hydrogen atoms were found by differences Fourier map. The final cycle of full matrix least-squares refinement was based on 1469 observed reflections ( $I > 2.5\sigma(I)$ ) and 246 variable parameters. Weights based on counting statistics were used. The maximum and minimum peaks on the final differences Fourier map corresponded to 0.220 and  $-0.230\text{ e/\AA}^3$ , respectively. All the calculations were performed using the NRCVAX crystallographic software package.<sup>41</sup>

**Molecular Modeling Calculations.** Molecular modeling calculations were performed with the semiempirical PM3 method implemented using the MOPAC package (Version 6.0) on a CAChe system run on a Macintosh IIfx. Geometries were optimized with the BFGS method as default.

Electronic absorption spectra were calculated at the ROHF level with the ZINDO package on the same system. The calculation was run with a configuration interaction setting of 9 and INDO/1 parameterization of the Hamiltonian.

**Acknowledgment.** The authors would like to thank Dr. C. Bensimon for carrying out the X-ray crystallographic experiments. Thanks are due to Dr. G. Facey for recording the NMR data and Dr. J. A. Ripmeester for allowing the use of the solid-state NMR facilities at the National Research Council of Canada. The authors would also like to thank the Natural Sciences and Engineering Research Council, the Networks of Centres of Excellence through the Mechanical and Thermomechanical Wood Pulps Network, and the Office of Basic Energy Sciences of the United States Department of Energy. Issued as NDRL-3642.

**Supplementary Material Available:** Complete crystallographic data for **IIa** (6 pages); list of observed and calculated structure factors (11 pages). Ordering information is given on any current masthead page.

(38) Wilkinson, F.; Kelly, G. In *Handbook of Organic Photochemistry*; Scaiano, J. C., Ed.; CRC Press: Boca Raton, FL, 1989; Vol. 1, p 293.  
(39) Patterson, L. K.; Lilie, J. *Int. J. Radiat. Phys. Chem.* 1974, 6, 129.

(40) Grant, D. F.; Gabe, E. J. *J. Appl. Crystallogr.* 1978, 11, 114.  
(41) Gabe, E. J.; Lee, F. L.; Lepage, Y. *J. Appl. Crystallogr.* 1989, 22, 384.